FLASH irradiation does not induce lipid peroxidation in liposomes containing cholesterol and α-tocopherol

Veljko Grilj[1*], Walther-Reiner Geyer[2], Pascal Froidevaux[1*]

[1]*Radiation Oncology Service, Oncology Department, Lausanne University Hospital and University of Lausanne, Lausanne, Switzerland*
[2]*Institute of Radiation Physics, Lausanne University Hospital and University of Lausanne, Lausanne, Switzerland*

*Corresponding authors: Veljko Grilj, veljko.grilj@chuv.ch and Pascal Froidevaux, pascal.froidevaux@chuv.ch

Conflict of interest/Disclosures: None

Funding: The study was supported the Swiss National Science Foundation grant n°10.004.987.

Data availability statement: Research data are stored in an institutional repository and will be shared upon reasonable request to the corresponding author.

Keywords: FLASH; lipid peroxidation; liposomes; cholesterol; tocopherol; EPR

Abstract

Background: A decrease in lipid peroxidation (LPO) under higher dose rate irradiation could play a role in the FLASH sparing effect. Our objective was to explore how LPO induced at FLASH (> 100 Gy/s) and conventional (CONV, < 10 Gy/min) dose rates in synthetic phospholipid membranes depends on concentrations of cholesterol (Chol) and α-tocopherol (Toc).

Materials and Methods: Solutions of phosphatidylcholine (PC) liposomes, either alone, with Chol or with a combination of Chol and Toc, were irradiated by FLASH and CONV electron beams. In addition, samples incorporating both Chol and Toc were tested under a range of gradually changing dose rates. LPO yield was assessed by oxygen consumption measurements and EPR spectrometry of spin probes (TEMPONE and mito-TEMPO).

Results: Regardless the cholesterol or tocopherol concentrations, LPO was considerably reduced when samples were irradiated at FLASH dose rates. Increasing Chol concentration led to a decrease in LPO yield upon irradiation, mostly likely due to the less oxidizing index of cholesterol compared with linoleic acid and increased stiffness of the membrane, hindering O_2 diffusion. Increasing Toc concentration led to an enhanced protection of the membrane from LPO. Increasing the average dose rate diminished the oxidative potential of the beam. EPR measurements demonstrated interaction of spin probes with membrane radicals in CONV, but not in FLASH.

Conclusions: Irradiation at FLASH dose rates was able to inhibit LPO in PUFA-containing artificial PC membranes under all tested conditions, demonstrating that the FLASH beam creates less oxidizing damage to a phospholipid membrane than a conventional beam.

1. Introduction

FLASH radiotherapy is an irradiation modality that uses ultra-high dose rates (UHDR, > 100 Gy/s). Compared to conventional irradiation (< 1 Gy/s), FLASH protects healthy tissues while being as efficient to control tumor progression.[1-4] Currently, the mechanism by which FLASH protects healthy tissues remains unclear, although radical-radical recombination is increasingly cited as a potential pathway for reducing levels of radiation induced reactive oxygen species (ROS) at UHDR.[5,6] Ionizing radiations are known to induce lipid peroxidation (LPO), which triggers ferroptosis, an iron-dependent non-apoptotic cell death.[7] In addition, radiation-induced LPO synergizes with ferroptosis inducers.[8] Lang et al. have demonstrated that radiotherapy and immunotherapy promoted tumor lipid oxidation through repression of the SLC7A11 system, a cysteine-glutamate transporter.[9] In cells, protection of the phospholipid membranes from LPO is essentially driven by the enzymatic GPx4 system, which uses glutathione as a co-factor to reduce reactive lipid hydroperoxides to harmless alcohol.[10] Thus, inactivation of GPx4 leads to extensive membrane LPO and ferroptosis.[11] While ferroptosis has been increasingly implicated in a host of diseases, the potential physiological functions of ferroptosis in tumour suppression and immune surveillance have also been emphasized.[12,13] Besides, the question of ferroptosis being potentially the key to unravel the enigma of the FLASH effect has been previously posed.[14,15] Recent developments have demonstrated that FLASH radiation abrogates lipid oxidase expression, as well as the generation of oxidized low-density lipid, to reduce PPARγ activity.[16] In contrast, conventional radiation induces reactive oxygen species-dependent PPARγactivation in macrophages. Therefore, reduction in LPO yield when increasing the dose rate in radiotherapy might be part of the FLASH effect by protecting healthy tissues from radiation-induced ferroptosis.

Recently, we demonstrated that a FLASH electron beam was not able to induce significant LPO in synthetic (liposomes) membranes.[15] To the opposite, conventional irradiation induced LPO linearly with the dose. In addition, we also demonstrated that the LPO yield in synthetic membranes was well correlated with the average dose rate, not the dose per pulse.[17] Combining these observations with the results from recent biological studies on FLASH radiotherapy and ferroptosis[9,11,13,16,18] we propose here a study on the effect of FLASH and conventional irradiation on the LPO of synthetic membranes containing Chol and Toc as a model of natural cell membranes. We determined LPO yield by measuring change in oxygen

level (ΔpO_2) during irradiation in both modalities using the phosphorescence quenching method[19] and EPR oximetry with lithium naphtalocyanine.[20] In addition, we used EPR spin probing with TEMPONE and mito-TEMPO to reveal the extend of the membrane peroxidation during irradiation. Results show that in all cases, CONV irradiation led to extended lipid peroxidation in our membrane model while FLASH was unable to induce similar reactions.

2. Material and Methods

2.1. Irradiation procedures

The irradiation setup and dosimetry followed the approach described in our earlier work.[17] In brief, irradiations were carried out with the Oriatron eRT6 LINAC (PMB Alcen), which produces a pulsed electron beam with energies of 5–6 MeV. Specific beam parameters for CONV and FLASH are provided in **Supplementary Table 1**. Liposome samples were placed in 1.75 mL glass vials, sealed, and positioned in a water bath at 10 mm water equivalent depth (mid-plane) using a custom-designed holder. Optical fibers attached to the vial enabled in situ oxygen monitoring during irradiation. The source-to-surface distance (SSD) was set by adjusting a movable platform supporting the water bath. Repetitive irradiations of PC liposome solutions containing different proportions of Chol, 7-dehydrocholesterol (7-DHC) and Toc were performed by delivering the total dose in steps of approximately 10 or 20 Gy for CONV and 40 Gy for FLASH. When pO_2 in the vial dropped below 20 mmHg, the steps were reduced to be able to accurately record the oxygen consumption G-value without fully depleting oxygen. In addition, a set of samples containing both Chol and Toc was exposed to gradually varying dose rates. In this experiment, the dose per pulse was fixed at 0.1 Gy, and different dose rates were achieved by adjusting the pulse repetition frequency (PRF).

Dosimetry employed GafChromic EBT3 films, an Advanced Markus ionization chamber, and an AC current transformer (ACCT) installed at the beam exit. The ionization chamber, corrected for saturation at high dose per pulse, was used for online dose verification prior to irradiations. EBT3 films, irradiated in water at 10 mm depth (corresponding to vial mid-plane), served to calibrate the ACCT signal, which was then used to determine the delivered dose for each vial.

2.2 Chemicals

Phosphatidycholine (PC) from soybean (60% in linoleic acid, 18:2), cholesterol (Chol), 7-dehydrocholesterol (7-DHC), α-tocopherol (Toc), potassium dihydrogenophosphate hexahydrate (KH_2PO_4), Chelex resin, potassium Chromium(III) tris-oxalato complex (CrOx),

chloroform, dichloromethane, hexane, and methanol (MeOH) were of analytical grade and purchased from Sigma Aldrich or Brunschwig Chemie (Switzerland). Superoxide dismutase (SOD) and mito-TEMPO were obtained from Sigma Aldrich (St-Louis, USA). TEMPONE was purchased from Cayman Chemical.

2.3 Phosphatidylcholine liposomes preparation

Phosphatidylcholine from soybean (PC 18:2) was purified immediately before liposome preparation. The purification process involved removal of phosphatidylethanolamine, tocopherol (along with other antioxidants), and various impurities, consisting mainly of free polyunsaturated fatty acids (PUFA) and saturated fatty acids. The purification was accomplished by chromatography on a silica gel (SiO_2) column using a PuriFlash XS520 apparatus (Advion-Interchim, France) and a gradient elution (MeOH in CH_2Cl_2, $10 \rightarrow 50\%$). To avoid lipids peroxidation, the UV cell was bypassed. The fractions containing PC were collected, the solvents were removed using a rotary evaporator, and the remaining solid was dried overnight under vacuum. The resulting pure PC was dissolved in $CHCl_3$, forming a stock solution for subsequent experiments. Cholesterol and tocopherol were also purified using SiO_2 column chromatography with CH_2Cl_2 as eluant for cholesterol, and hexane:CH_2Cl_2 1:1 for tocopherol. To achieve the final composition of the various liposomal formulations, adequate aliquots of PC (18:2 60%), Chol, 7-DHC and Toc in $CHCl_3$ stock solutions were weighted and mixed. The solvent was removed on a rotary evaporator, and the lipids film was dried under vacuum for at least two hours. Subsequently, phosphate buffer (5 mM, pH 7.4) was added to reach a desired concentration of PC (10 - 20 mM for ΔpO_2 measurements or 200 mM for spin probing experiments). The mixture was left for one hour to wet and then was subjected to sonication for one minute. The obtained cloudy solution was vortexed thoroughly and extruded ten times under pressurized N_2 (5 bars) through a polycarbonate membrane (100 nm average pore size) using a Genizer JGE-100 mL liposome extruder (Genizer LLC, CA, USA) for volumes above 10 mL or with a mini-extruder for volumes below 10 mL (Avanti Research). However, when liposomes at PC concentration of 200 mM contained high percentage of cholesterol or 7-DHC, the stiffness of the membranes was such that it was only possible to extrude them at 200 nm. The resulting liposomes were stored at 4°C and used within 24 h. The size distribution of the liposomes was determined by dynamic light scattering using a Delsa Nano C apparatus (Beckman-Coulter). The liposomes were found to exhibit an average diameter of 130 ± 2.0 nm (PC:Chol 3:1, PC:Toc 500:1) and 139 ± 3.0 (PC:Chol 3:1) and a

polydispersity index of 0.08. In all experiments, irradiations were conducted using liposome solutions that were equilibrated with air (containing 21% O_2), except when specifically mentioned.

2.3.1 Reduction of lipids hydroperoxides with Ph_3P and reduction of metals concentration with Chelex

To minimise the role of the Fenton's reaction in our experiments, lipids hydroperoxides were reduced in alcohol with Ph_3P and the phosphate buffer was kept on Chelex resin to remove all metals. Briefly, in a 50 mL glass balloon, 500 mg of raw PC was dissolved in methanol (10 mL) and Ph_3P (50 mg) was added. The solution was warmed at 40°C for ½ h. After cooling, PC was purified on SiO_2 as described above. To remove metals, a 50 mM phosphate buffer was prepared in 50 mL ultrapure water in a plastic vial. 1 g of Chelex resin was added and the vial was vortexed from time to time over at least 3 days. From this vial, a fraction was taken for preparing a 5 mM phosphate buffer at pH 7.4. Lipid films were then hydrated with phosphate buffer to enable liposome formation. However, experiments with varying Chol and Toc proportions, as well as those conducted at different dose rates, were repeated using liposomes not pretreated with Ph_3P and buffer not processed through Chelex resin, to evaluate the influence of these procedures on LPO yields.

2.4 Assessment of lipid peroxidation

Oxygen phosphorescence quenching: oxygen concentration in sealed vials subjected to irradiation was measured by the phosphorescence quenching method, using molecular oxygen probe Oxyphor PtG4 (1 µM) and a commercial fiber-optic phosphorometer (Oxyled, Oxygen Enterprises), as described previously.[17,19] The lifetime of the phosphorescence emitted by the probe, which was dissolved directly in the medium, is dependent on the oxygen partial pressure (pO_2) in the medium. pO_2 was recorded (in units of mmHg) before, during, and after irradiation with a measurement frequency of 1 Hz. The amount of oxygen consumed during irradiation of liposome samples was determined as the difference (ΔpO_2) in oxygen levels before and immediately after irradiation and expressed in units of mmHg. Calculated ΔpO_2 values were finally divided by the corresponding dose to obtain the oxygen consumption G-values (in mmHg/Gy) which serves as a proxy for the LPO yield.

EPR oximetry with lithium naphtalocyanine (LiNc): LiNc was synthesized as described by Pandian et al.[20] The calibration of the LiNc EPR linewidth as a function of the concentration of molecular oxygen was conducted using independent O_2 concentration measurements with an

OxyLite Pro XL instrument (Oxford Optronix, UK). For EPR oximetry with liposomes, 3.5 mg of LiNc was suspended in 2 ml EtOH, vortex for 1 minute and centrifuged (13'000 rnd/min) for 3 minutes. This operation was repeated twice with EtOH and twice with the phosphate buffer (10 mM). Afterwards, LiNc crystals were resuspended in 2 ml phosphate buffer. 5 µL of this suspension was added to 50 µL of the liposome preparation. The mixture was introduced in a 50 µL capillary sealed at both extremities with wax, ensuring that no air was introduced. After determining the initial pO_2 (linewidth 4.21 G, ~154 mm Hg), the capillary was irradiated inside the water tank followed by another EPR measurement of pO_2. Irradiations and EPR measurements were repeated until pO_2 reached 0 mmHg (linewidth 0.469 G). EPR signals were recorded using a Bruker EMX Nano spectrometer (Bruker, Germany) situated close to the irradiation bunker, thus allowing a rapid transfer of the sample from the irradiation setup to the EPR spectrometer. Recording parameters included: centre field of 3444 G, field width of 50 G, scan time of 30 s, 2-5 scans, receiver gain of 40 dB, amplitude modulation of 0.2 G, and 10 dB attenuation (10 mW microwave power).

2.5 EPR spectrometry using TEMPONE and mito-TEMPO spin probes

We used TEMPONE and mito-TEMPO to target the lipid membrane with an EPR active probe which will react with lipid radicals inside the membrane, e.g. lipid peroxyl radicals (LOO•) resulting in a diminution of the spin probe EPR signal. TEMPONE is a spin probe which will be dispersed in every compartment of the liposome solution (buffer, membrane and inner liposome volume). Mito-TEMPO, bearing a triphenyl phosphonium group (Ph_3P^+) is more lipophilic and targets the lipid membrane. TEMPONE or mito-TEMPO were added at a final concentration between 1.2 and 10 µM to PC liposomes solution (200 mM). Potassium Chromium(III) tris-oxalato complex (CrOx, 20 mM) was added as a spin-spin relaxing agent (line broadening agent) allowing visualisation of the EPR signals coming only from the membrane and the inner liposome volume.[21] Impact of CrOx on EPR signal from liposome solutions containing TEMPONE and mito-TEMPO was tested by recording the spectrum before and after the addition of CrOx. For irradiations, the mixture containing liposomes, CrOx and one of the spin probes was introduced inside the EPR cavity in the flow-through cell geometry. After recording the spectrum, the mixture was retrieved, introduced into a 0.5 mL Eppendorf tube, irradiated, and then measured again. The operation was repeated until a given cumulative dose was reached, depending upon the liposomes formulation. Recordings were performed with the following parameters: centre field of 3440 G, field width of 100 G, scan

time of 60 s, amplitude modulation of 1 G, 2-5 scans, receiver gain of 40 dB, and 10 dB attenuation (10 mW microwave power).

3. Results

3.1 LPO yield is reduced by the presence of Chol and Toc

LPO yield expressed as ΔpO_2/Gy was recorded during consecutive irradiations of various liposomes formulations until oxygen was fully depleted from the vial ($pO_2 \sim 0$ mm Hg). Dependances of obtained ΔpO_2/Gy values on cumulative dose are shown in **Figure 1**. Liposome solutions containing Chol revealed that increase in Chol concentration negatively affected the LPO yield during CONV irradiation (**Fig. 1A, C**). This effect was even more pronounced when Chol was replaced by 7-DHC. In addition, we observed an increase in ΔpO_2/Gy starting from around 1 mm Hg/Gy to over 3 mm Hg/Gy during the overall irradiation process. Under FLASH, all liposome formulations produced considerably lower LPO yields than under CONV. Differences in LPO yield among various liposome formulations exposed to FLASH were minimal. These results were confirmed with LiNc EPR oximetry, demonstrating that the phosphorescence quenching method used for oxygen measurements did not interfere with the LPO process (**Supplementary Fig. S1**).

Incorporation of Toc into the liposomes diminished initial LPO yields following CONV irradiation, revealing the protective effect of Toc in reducing membrane oxidative damage (**Fig. 1B, D**). As cumulative dose increased, progressive oxidation of Toc molecules led to a rise in LPO yield, which peaked just before complete depletion of oxygen in the sample. Samples with higher Toc concentrations required a greater cumulative dose before showing an increase in LPO yield. Therefore, the dose needed for complete oxygen depletion increased from 145 Gy in liposomes with a PC:Toc ratio of 1:2000 to 420 Gy in liposomes with a PC:Toc ratio of 1:200. FLASH irradiation did not induce notable LPO, regardless of Toc content and doses up to 750 Gy were necessary to fully deplete oxygen in the vessels, comparable to pure buffer (5 mM K_2HPO_4, pH 7.4). Liposomes prepared without Ph_3P pretreatment and with phosphate buffer that had not been processed through Chelex resin reproduced similar results (**Fig. 1C, D**), demonstrating that initial lipid hydroperoxides, if present, were low in concentration and did not play a significant role in our experiments. The same conclusion applies with respect to the metal content. However, to stay on the safe side and keep initial lipid hydroperoxides' and metals' contents as low as possible, PC was treated with Ph_3P before

purification and the phosphate buffer was preserved on Chelex in all our experiments. This ensured greater reproducibility among liposome batches and minimized the contribution of the Fenton reaction, allowing the effects of irradiation to be isolated.

3.2 LPO yield depends on cumulative dose, not on the baseline pO_2

Given the progressive increase in LPO yield with cumulative dose, accompanied by a concurrent decline in pO_2 within the vial, we investigated whether LPO yield is dependent on oxygen tension. To this end, liposome suspensions were deoxygenated by repeated vacuum/N_2 cycles and subsequently re-oxygenated by air diffusion providing samples with varying baseline pO_2 (designated as "Hypoxic1-6" in **Fig. 2**). The initial O_2 consumption G-values (corresponding to cumulative dose of 0 Gy) were comparable across baseline pO_2 values ranging from 16 to 147 mmHg, while the rise in G-values during repetitive irradiation was consistently reproduced regardless of the baseline pO_2 (**Fig. 2A**). This trend is most clearly illustrated when O_2 consumption G-values are plotted against cumulative dose (**Fig. 2B**). All samples followed a similar linear increase while pO_2 was above 40–50 mmHg. As pO_2 dropped below this range, the increase in G-values stalled and ultimately reversed just before total oxygen depletion.

When the suspension was pre-irradiated with 100 Gy to deplete oxygen and subsequently re-oxygenated to ≈150 mmHg, the initial G-value changed significantly, from just under 1.0 mmHg/Gy in non-irradiated solutions to nearly 2.5 mmHg/Gy. Furthermore, in these pre-irradiated samples, the LPO showed minimal further increase during subsequent irradiation steps. Next, we tested whether rise in LPO yields could be attributed to the accumulation of water radiolysis products such as superoxide (O_2•–) or hydrogen peroxide (H_2O_2). Pretreatment of liposomes with SOD prior to irradiation led to higher LPO yields (**Fig. 2**). Nevertheless, the cumulative dose effect on LPO yield remained. Finally, liposome suspensions supplemented with H_2O_2 at a concentration equivalent to that generated by 100 Gy irradiation of pure water (10 µM) showed LPO yields identical to those of untreated samples.

3.3 Increasing the DR_{av} lowers the radiation's oxidative impact on liposomes containing Chol and Toc

Liposome preparations containing both Chol and Toc at PC:Chol 3:1 and PC:Toc 1000:1 ratios were submitted to irradiation across a range of DR_{av}, ranging from CONV to FLASH conditions. Measured ΔpO_2/Gy values are shown as function of the cumulative dose for each DR_{av} in

Figure 3. The cumulative dose needed for complete oxygen depletion increased progressively with DR_{av} (**Fig. 3A**). Similar results were reproduced in non-reduced PC liposomes prepared using buffer not preserved on Chelex (**Fig. 3B**).

3.4 Spin probing of the radiation induced membrane radicals

3.4.1. Impact of CrOx on EPR spectra of TEMPONE and mito-TEMPO dissolved in PC liposome solutions.

Measurement of EPR spectra before and after the addition of CrOx (20 mM) to PC liposome solutions (200 mM) containing either TEMPONE (6 µM) or mito-TEMPO (2.5 µM) revealed a >90% decrease in signal for TEMPONE, but only ~40% for mito-TEMPO. This indicates that mito-TEMPO predominantly resides within the phospholipid bilayer, whereas TEMPONE is distributed throughout the solution (**Supplementary Fig. S2**).

3.4.1 Scavenging effects of spin-probes at higher probe concentrations

Nitroxide spin probes such as TEMPONE and mito-TEMPO can function as chain-breaking antioxidants, readily reacting with nearby radicals to form diamagnetic adducts. For lipid radicals generated by radiation within liposomes, this scavenging effect was expected to be particularly pronounced for mito-TEMPO due to its strong affinity for the lipid phase. Irradiation of PC liposome solutions containing 5 µM of TEMPONE or mito-TEMPO with 80 Gy CONV resulted in an almost complete loss of the TEMPONE signal, whereas only a slight decrease in mito-TEMPO signal intensity was observed (**Fig. 4A, B**), indicating that at this concentration the antioxidative action of mito-TEMPO predominated. However, when the mito-TEMPO concentration was reduced to 1.25 µM, a marked decrease in its EPR signal was detected at the same dose (**Fig. 4C**), suggesting that at lower concentrations the scavenging efficiency of mito-TEMPO diminished while its direct reduction increased. FLASH irradiation caused no detectable change in signal intensity, regardless of the spin probe type or concentration (data not shown). To better isolate the signal arising from probes embedded within the lipophilic membrane region, CrOx broadening agent was added to the buffer prior to liposome formation, thereby suppressing spin-probe signals originating from the inner liposome volume. Although this approach allowed a more accurate assessment of the role of spin probes as radical scavengers, it was not used in other experiments to avoid potential membrane oxidation caused by the transition metals present in CrOx. Instead, CrOx was added to the liposome suspension immediately before the EPR measurements. Consequently, a portion of the TEMPONE or mito-TEMPO EPR signal originated from probes located within the

inner liposome volume. Finally, based on these results, most mito-TEMPO measurements were conducted at a concentration of 2.3 µM, which provided a stronger EPR signal while still allowing lipid peroxidation to propagate throughout the membrane.

3.4.2 TEMPONE EPR signal intensity is reduced after CONV but not after FLASH

EPR spectra of liposome solutions containing the TEMPONE spin probe and CrOx broadening agent were recorded before and immediately after irradiation by both CONV and FLASH modalities. N-oxyl spectra were characterized by N-hyperfine coupling leading to 3 lines of the same intensity. However, when partitioned between an aqueous and a lipid phase, the high field line was split, being the result of less rotational freedom degree in the lipid membrane. Results showed that for PC liposome preparations containing pure PC, Chol (PC:Chol 3:1) or 7-DHC (PC:7-DHC 3:1), an 80 Gy CONV irradiation induced a significant reduction in TEMPONE EPR signal (left panels in **Fig. 5A, B, C**). To the opposite, 80 Gy FLASH had no influence on the TEMPONE signal (right panels in **Fig. 5A, B, C**). However, when one molecule of Toc was added per 1000 PC molecules (PC:Toc 1000:1) in PC:Chol 3:1 preparation, the TEMPONE EPR signal remained unchanged even after receiving 80 Gy of CONV (**Fig. 5D left**). Slight reduction in signal intensity was observed only above 320 Gy (data not shown). Once again, FLASH had no impact on the EPR signal intensity (**Fig. 5D right**).

3.4.3 mito-TEMPO ERP signal intensity is reduced after CONV but not after FLASH

EPR spectrum of mito-TEMPO showed broader hyperfine line compared with TEMPONE because most of the probe is in the lipophilic membrane, restricting rotational motion. The high field hyperfine line had broadened to such an extent that it almost disappeared from the spectrum. As in the TEMPONE experiments, EPR spectra of liposome solutions containing the mito-TEMPO spin probe and CrOx broadening agent were taken right before and after irradiation with CONV and FLASH. Repetitive delivery of 20 Gy CONV resulted in progressive depletion of mito-TEMPO EPR signal up to 100 Gy cumulative dose, while no change in EPR spectra occurred up to 80 Gy in FLASH (**Fig. 6A**). Slight signal diminution with FLASH was observed only after exceeding 100 Gy. Similarly, 80 Gy CONV irradiation of PC liposomes containing Chol (PC:Chol 3:1) or 7-DHC (PC:7-DHC 3:1) provoked a significant decrease in mito-TEMPO EPR signal (left panels in **Fig. 6B, C**) while no decrease was observed after 80 Gy of FLASH (left panels in **Fig. 6B, C**). However, when Toc was added into PC liposome composition together with Chol (PC:Chol 3:1, PC:Toc 1000:1), both FLASH and CONV were unable to affect the mito-TEMPO EPR signal (**Fig. 6D**).

4. Discussion

4.1 Impact of Chol and 7-DHC on LPO process

Oxygen, as a small and neutral molecule, may permeate the plasma membrane through lipid bilayer leaflets.[22] However, using molecular dynamics calculations, Wennberg et al.[23] and Boonoy et al.[24] demonstrated that increasing the Chol content of membrane led to reduced transfer of small molecules (such as O_2) across the membrane and to an increased membrane rigidity, reducing the O_2 partition coefficient. In our experiments, increasing the Chol content of the membrane reduced the LPO yield induced by CONV in pure PC samples (**Fig. 1A, C**). This effect may be due to the rate constant of lipid peroxidation propagation (k_p), which is smaller for Chol (k_p = 11 M^{-1} s^{-1}) than for linoleic acid (k_p = 62 M^{-1} s^{-1}) and/or to the increase in stiffness of the membrane with the cholesterol content,[22] reducing oxygen diffusion inside the membrane where polyunsaturated fatty acids (PUFA) are present. In contrast, 7-DHC possesses the highest k_p among known lipids (2260 M^{-1} s^{-1}), indicating its high intrinsic reactivity toward peroxyl radicals. Interestingly, PC liposomes containing 7-DHC showed an initial LPO yield comparable to that of Chol-containing liposomes. However, the LPO yield in 7-DHC containing liposomes remained essentially unchanged with increasing cumulative dose, whereas in liposomes containing Chol it continued to rise. Recently, Freitas et al.[25] and Li et al.[26] have demonstrated the role of 7-DHC in dictating ferroptosis. In brief, both studies demonstrated that the conjugated diene of 7-DHC exert high reactivity towards peroxyl radicals, effectively protecting (phospho)lipids from autoxidation and subsequent fragmentation. Conversely, the 7-DHC reductase (DHCR7), the enzyme which reduces 7-DHC to Chol, exerts a pro-ferroptosis action.[25,26] Our results indicate that 7-DHC acts as a protective molecule for the membrane, lowering radiation induced LPO yield and thereby supporting its proposed anti-ferroptotic role.

4.2 Increase in LPO yield with cumulative dose

Repetitive irradiation of PC liposomes, with or without Chol, resulted in progressive rise in LPO yield that continued until oxygen within the vials was nearly depleted (**Fig. 1A,C**). Since the pO_2 in the vials decreased in parallel, we initially hypothesized that this increase reflected a dependence on oxygen availability. However, this explanation was ruled out by the observation of comparable initial LPO yields across liposome suspensions pre-equilibrated at varying oxygen tensions, indicating that the LPO yield in non-irradiated solution is not pO_2

dependent (**Fig. 2A**). Indeed, the consistent increase in LPO with cumulative dose was observed irrespective of baseline pO_2 (**Fig. 2B**), suggesting that the effect is more likely driven by cumulative radiation-induced chemistry, such as the accumulation of lipid-derived radicals or secondary reactive species, rather than by oxygen concentration alone. In fact, below approximately 50 mmHg pO_2, further increase in LPO slows down, demonstrating that oxygen availability limits LPO at low concentrations. Pretreatment of liposome samples with SOD enhanced absolute LPO yields, likely by suppressing the scavenging effect of O_2•– generated in solution (**Fig. 2**). However, it did not qualitatively affect the dose-dependent increase in LPO. Additionally, H_2O_2 supplementation had no effect on the results. Taken together, these findings indicate that the accumulation of reactive species such as O_2•– and H_2O_2 does not account for the observed rise in LPO yields. In contrast, when liposome suspensions were first irradiated with 100 Gy and subsequently re-oxygenated, the initial LPO yield increased by 2.5-fold, with only a minor further rise thereafter. This suggests that membrane damage accumulated during repetitive CONV irradiations was driving the increase in LPO yield and that after a certain dose the liposome might be fully destroyed. Within the time frame of our irradiations, phospholipid damage primarily included the formation of lipid hydroperoxyl radicals and hydroperoxides. Compared to their PUFA precursors, these products are more hydrophilic, and the hydroperoxide-bearing lipophilic tails tend to bend toward the membrane surface[27]. This structural change increases membrane disorder and exposes PUFA residues to water radiolysis-derived radicals (e.g., HO•), thereby accelerating LPO reaction. Additional membrane disruption may also arise from lipid fragmentation following oxygen addition and/or cyclic endoperoxide formation. This mechanism is backed by our finding that 7-DHC acted as a protector of the membrane against peroxidation. Due to the presence of a diene within the B-ring of the sterol structure, oxidation of 7-DHC yields oxysterols without causing fragmentation or generating secondary radicals, thereby preserving membrane integrity.[25-27]

Our findings indicate that CONV irradiation promotes structural alterations in the membrane that increase its susceptibility to oxidation, an effect particularly relevant in the context of ferroptosis, where the buildup of lipid hydroperoxides plays a central role in driving cell death. In this context, the time scale of dose delivery is critical because lipid rearrangements and

fragmentation require time to develop. Thus, the ultrashort delivery of FLASH may be insufficient for such membrane-damaging processes to occur during the irradiation.

4.3. Tocopherol protects liposome membrane from lipid peroxidation

Toc is the main antioxidant present in biological phospholipid membranes, acting through the formation of a relatively stable chromanoxyl radical.[28,29] Introducing Toc into liposome membranes provided clear protection against lipid peroxidation during CONV irradiation (**Fig. 1B, D**). This effect reflects Toc's established role as a chain-breaking antioxidant, interrupting lipid radical propagation. By increasing the Toc content from 1:2000 to 1:200 (Toc:PC), nearly a threefold higher cumulative dose was needed to fully deplete oxygen under CONV. Under FLASH conditions, however, the effect of Toc remained modest with the cumulative dose required for complete oxygen depletion increased by only 15% between the lowest and highest Toc levels, indicating that FLASH induces minimal chain propagation.

4.4. Dependence of LPO process on average dose rate

The liposome formulation with PC:Chol at a 3:1 and PC:Toc at a 1000:1 ratio was chosen as our "gold standard," as it closely mirrors the typical Chol and Toc composition of cellular membranes.[30,31] When samples of this formulation were irradiated over a range of dose rates, increasing the dose rate progressively reduced the dose-dependent rise in LPO yield and increased the total dose required for full oxygen depletion (**Fig. 3**). This trend points again to a diminished capacity of high dose-rate irradiation to sustain oxidative processes within the liposome membrane. Interestingly, the effect of higher dose rates closely mirrored that of increased Toc levels, clearly illustrating that FLASH irradiation may promote radical chain-breaking processes, potentially by enhancing rapid radical recombination and favoring the formation of more stable species.

4.5 Spin-probing of radical interactions in the membrane.

By employing spin probes that localize within the lipid membrane, we were able to selectively probe radical–radical interactions confined to the allylic PUFA chains. Since radical termination requires another radical, the decay in EPR intensity of stable probes like TEMPONE and mito-TEMPO specifically reflects such inter-radical reactions. To increase the sensitivity of the method, a line broadening agent (CrOx) which does not cross the membrane was used to relax EPR signal originating outside of the liposomes. Our results show that CONV irradiation induced substantial rate of interactions between radicals and spin probes within the membrane, as evidenced by a decrease in EPR signal intensity for both TEMPONE and

mito-TEMPO. In contrast, FLASH irradiation produced no detectable radical–spin probe interactions, closely resembling the results observed when the radical scavenger Toc was present within the membrane. Spin-probe results therefore confirm our previous observations and support the proposed mechanism in which radical formation and/or propagation within the membrane is drastically reduced under FLASH dose rates.

6. Conclusions

Our study demonstrated that, unlike CONV irradiation, FLASH fails to trigger pro-ferroptotic LPO in synthetic membranes containing the primary components of biological membranes. While the precise mechanism limiting peroxidation process remains debated, conducted EPR spin-probing experiments revealed that radical propagation occurs within the lipophilic region of the membrane under CONV irradiation, but not under FLASH. We also showed that Toc functions as a chain-breaking antioxidant, although this membrane protection can be overcome by increasing the dose under CONV conditions. Notably, increasing the average dose rate led to a decrease in LPO yield like that observed at higher proportions of Toc, suggesting that reduction of ferroptosis in healthy tissues may contribute to the FLASH effect. The rationale for clinical translation of FLASH is based on its protective effect in normal tissues while maintaining comparable tumor control to CONV irradiation. High proton and iron content, hallmarks of the tumor microenvironment (TME), favor Fenton chemistry and ferroptosis. In this context, FLASH may still induce some lipid peroxidation, potentially affecting ferroptosis and tumor control. Indeed, a recent study by Vilaplana-Lopera et al.[30] reported that FLASH increases lipid peroxidation and induces ferroptosis in tumor cells, while sparing normal tissues. Importantly, mice on a high-iron diet exhibited a reversal of FLASH's protective effect, suggesting that baseline iron levels and iron-driven lipid peroxidation are critical factors defining biological outcomes following FLASH.

6. Acknowledgement

The study was supported by grants of the Swiss National Science Foundation grant n°10.004.987.

Declaration of generative AI and AI-assisted technologies in the manuscript preparation process

During the preparation of this work the authors used Gemini Pro for text editing. After using this tool/service, the authors reviewed and edited the content as needed and take full responsibility for the content of the published article.

References:

1. Favaudon V, Caplier L, Monceau V, et al. Ultrahigh dose-rate FLASH irradiation increases the differential response between normal and tumor tissue in mice. *Science Translational Medicine* 2014; **6**(245).
2. Montay-Gruel P, Acharya MM, Petersson K, et al. Long-term neurocognitive benefits of FLASH radiotherapy driven by reduced reactive oxygen species. *Proceedings of the National Academy of Sciences of the United States of America* 2019; **116**(22): 10943-51.
3. Montay-Gruel P, Petersson K, Jaccard M, et al. Irradiation in a flash: Unique sparing of memory in mice after whole brain irradiation with dose rates above 100 Gy/s. *Radiotherapy and Oncology* 2017; **124**(3): 365-9.
4. Vozenin MC, Bourhis J, Durante M. Towards clinical translation of FLASH radiotherapy. *Nature Reviews Clinical Oncology* 2022; **19**(12): 791-803.
5. Kusumoto T, Kitamura H, Hojo S, Konishi T, Kodaira S. Significant changes in yields of 7-hydroxy-coumarin-3-carboxylic acid produced under FLASH radiotherapy conditions. *Rsc Advances* 2020; **10**(63): 38709-14.
6. Labarbe R, Hotoiu L, Barbier J, Favaudon V. A physicochemical model of reaction kinetics supports peroxyl radical recombination as the main determinant of the FLASH effect. *Radiotherapy and Oncology* 2020; **153**: 303-10.
7. Lei G, Zhang YL, Koppula P, et al. The role of ferroptosis in ionizing radiation-induced cell death and tumor suppression. *Cell Research* 2020; **30**(2): 146-62.
8. Ye LF, Chaudhary KR, Zandkarimi F, et al. Radiation-Induced Lipid Peroxidation Triggers Ferroptosis and Synergizes with Ferroptosis Inducers. *Acs Chemical Biology* 2020; **15**(2): 469-84.
9. Lang XT, Green MD, Wang WM, et al. Radiotherapy and Immunotherapy Promote Tumoral Lipid Oxidation and Ferroptosis via Synergistic Repression of SLC7A11. *Cancer Discovery* 2019; **9**(12): 1673-85.
10. Dixon SJ, Stockwell BR. The Hallmarks of Ferroptosis. In: Jacks T, Sawyers CL, eds. Annual Review of Cancer Biology, Vol 3; 2019: 35-54.
11. Alves F, Lane D, Nguyen TPM, Bush AI, Ayton S. In defence of ferroptosis. *Signal Transduction and Targeted Therapy* 2025; **10**(1).
12. Jiang XJ, Stockwell BR, Conrad M. Ferroptosis: mechanisms, biology and role in disease. *Nature Reviews Molecular Cell Biology* 2021; **22**(4): 266-82.
13. Dierge E, Debock E, Guilbaud C, et al. Peroxidation of n-3 and n-6 polyunsaturated fatty acids in the acidic tumor environment leads to ferroptosis-mediated anticancer effects. *Cell Metabolism* 2021; **33**(8): 1701-+.
14. Vilaplana-Lopera N, Abu-Halawa A, Walker E, Kim J, Moon EJ. Ferroptosis, a key to unravel the enigma of the FLASH effect? *British Journal of Radiology* 2022; **95**(1140).
15. Froidevaux P, Grilj V, Bailat C, Geyer WR, Bochud F, Vozenin MC. FLASH irradiation does not induce lipid peroxidation in lipids micelles and liposomes. *Radiation Physics and Chemistry* 2023; **205**.
16. Ni HW, Reitman ZJ, Zou W, et al. FLASH radiation reprograms lipid metabolism and macrophage immunity and sensitizes medulloblastoma to CAR-T cell therapy. *Nature Cancer* 2025.
17. Grilj V, Paisley R, Sprengers K, et al. Average dose rate is the primary determinant of lipid peroxidation in liposome membranes exposed to pulsed electron FLASH beam. *Radiation Physics and Chemistry* 2024; **222**.
18. Vilaplana-Lopera N, Kim J, Nam G, et al. Tissue-specific iron levels modulate lipid peroxidation and the FLASH radiotherapy effect. *Cell Death & Disease* 2025; **16**(1).
19. Esipova TV, Barrett MJP, Erlebach E, Masunov AE, Weber B, Vinogradov SA. Oxyphor 2P: A High-Performance Probe for Deep-Tissue Longitudinal Oxygen Imaging. *Cell Metabolism* 2019; **29**(3): 736-+.

20. Pandian RP, Dolgos M, Marginean C, et al. Molecular packing and magnetic properties of lithium naphthalocyanine crystals: hollow channels enabling permeability and paramagnetic sensitivity to molecular oxygen. *Journal of Materials Chemistry* 2009; **19**(24): 4138-47.
21. Samuni A, Carmichael AJ, Russo A, Mitchell JB, Riesz P. ON THE SPIN TRAPPING AND ELECTRON-SPIN-RESONANCE DETECTION OF OXYGEN-DERIVED RADICALS GENERATED INSIDE CELLS. *Proceedings of the National Academy of Sciences of the United States of America* 1986; **83**(20): 7593-7.
22. Zuniga-Hertz JP, Patel HH. The Evolution of Cholesterol-Rich Membrane in Oxygen Adaption: The Respiratory System as a Model. *Frontiers in Physiology* 2019; **10**.
23. Wennberg CL, van der Spoel D, Hub JS. Large Influence of Cholesterol on Solute Partitioning into Lipid Membranes. *J Am Chem Soc* 2012; **134**(11): 5351-61.
24. Boonnoy P, Janlad M, Bagheri B, Dias C, Karttunen M, Wong-ekkabut J. Cholesterol inhibits oxygen permeation through biological membranes: mechanism against double-bond peroxidation. *Rsc Advances* 2024; **14**(40): 29113-21.
25. Freitas FP, Alborzinia H, dos Santos AF, et al. 7-Dehydrocholesterol is an endogenous suppressor of ferroptosis. *Nature* 2024; **626**(7998).
26. Li YX, Ran Q, Duan QH, et al. 7-Dehydrocholesterol dictates ferroptosis sensitivity. *Nature* 2024; **626**(7998).
27. Xu LB, Korade Z, Porter NA. Oxysterols from Free Radical Chain Oxidation of 7-Dehydrocholesterol: Product and Mechanistic Studies. *J Am Chem Soc* 2010; **132**(7): 2222-32.
28. Buettner GR. THE PECKING ORDER OF FREE-RADICALS AND ANTIOXIDANTS - LIPID-PEROXIDATION, ALPHA-TOCOPHEROL, AND ASCORBATE. *Archives of Biochemistry and Biophysics* 1993; **300**(2): 535-43.
29. Fukuzawa K. Dynamics of lipid peroxidation and antioxidion of α-tocopherol in membranes. *Journal of Nutritional Science and Vitaminology* 2008; **54**(4): 273-85.
30. Kelley EE, Buettner GR, Burns CP. RELATIVE ALPHA-TOCOPHEROL DEFICIENCY IN CULTURED-CELLS - FREE RADICAL-MEDIATED LIPID-PEROXIDATION, LIPID OXIDIZABILITY, AND CELLULAR POLYUNSATURATED FATTY-ACID CONTENT. *Archives of Biochemistry and Biophysics* 1995; **319**(1): 102-9.
31. Evarts RP, Bieri JG. RATIOS OF POLYUNSATURATED FATTY-ACIDS TO ALPHA-TOCOPHEROL IN TISSUES OF RATS FED CORN OR SOYBEAN OILS. *Lipids* 1974; **9**(11): 860-4.

Figure captions:

Figure 1. Oxygen consumption G-value (used as proxy for LPO yield) as a function of cumulative dose in: (A, C) PC liposome solutions (10 mM) containing varying concentrations of Chol or 7-DHC; and (B, D) PC liposome solutions (10 mM) containing Chol at a PC:Chol ratio of 3:1 with different concentrations of Toc. Samples in (A) and (B) were prepared using Ph_3P-reduced liposomes and Chelex-treated buffer, whereas samples in (C) and (D) were prepared without Ph_3P reduction and with buffer not treated with Chelex resin.

Figure 2. Oxygen consumption G-values (serving as a proxy for LPO yield) are plotted as a function of (A) pO_2 at the start of each irradiation step and (B) cumulative dose reached before each irradiation step. Experiments used 10 mM PC liposome solutions prepared under various conditions: at room pO_2 with or without addition of SOD or H_2O_2, pre-equilibrated at different oxygen levels (Hypoxic 1–6), or pre-irradiated at 100 Gy and reoxygenated. Colors distinguish different samples. In panel (A), the data point with the highest pO_2 for each sample represents the initial irradiation (0 Gy cumulative dose). The progression of cumulative dose during sequential irradiation is explicitly highlighted for the 'Hypoxic4' sample.

Figure 3. Effect of the average dose rate (DR_{av}) on oxygen consumption G-values as a function of cumulative dose in PC liposomes containing both Chol and Toc at PC:Chol and PC:Toc molar ratios of 3:1 and 1000:1, respectively. (A) Ph_3P-reduced liposomes with Chelex-treated buffer; (B) liposomes without Ph_3P reduction prepared in non-Chelex-treated buffer.

Figure 4. EPR spectrum of PC liposome samples containing (A) 5 μM TEMPONE, (B) 5 μM mito-TEMPO and (C) 1.25 μM mito-TEMPO before (black line) and after (blue dotted line) irradiation with 80 Gy CONV.

Figure 5. TEMPONE EPR spectra before (black line) and after 80 Gy CONV (left, dotted blue line) or 80 Gy FLASH (right, dotted red line) irradiation of PC liposomes (200 mM) containing (A) pure PC, (B) Chol at PC:Chol 3:1, (C) 7-DHC at PC:7-DHC 3:1; (D) Chol and Toc at PC:Chol 3:1, PC:Toc 1000:1. CrOx (20 mM) was added to all samples before recording the first EPR spectrum.

Figure 6. (A) Mito-TEMPO EPR spectra before (black line) and after successive 20 Gy CONV (left) or 20 Gy FLASH (right) irradiations of PC liposomes (200 mM) containing pure PC. (B) Mito-TEMPO EPR spectra before (black line) and after 80 Gy CONV (left, dotted blue line) or

80 Gy FLASH (right, dotted red line) irradiation of PC liposomes (200 mM) containing Chol at PC:Chol 3:1. (C) same as (B) but for PC liposomes containing 7-DHC at PC:7-DHC 3:1. (D) same as (B) but for PC liposomes containing Chol and Toc at PC:Chol 3:1, PC:Toc 1000:1. CrOx (20 mM) was added to all samples before recording the first EPR spectrum.

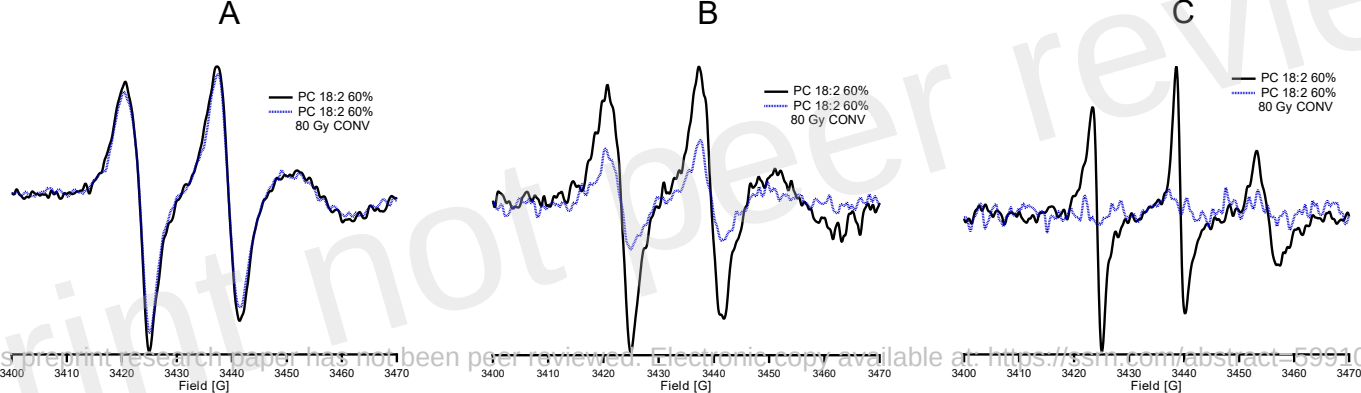

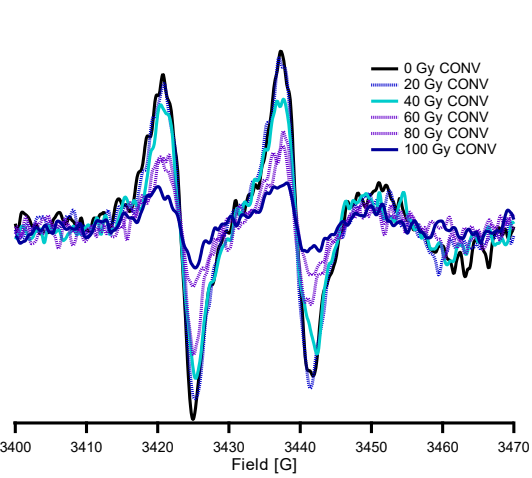

A

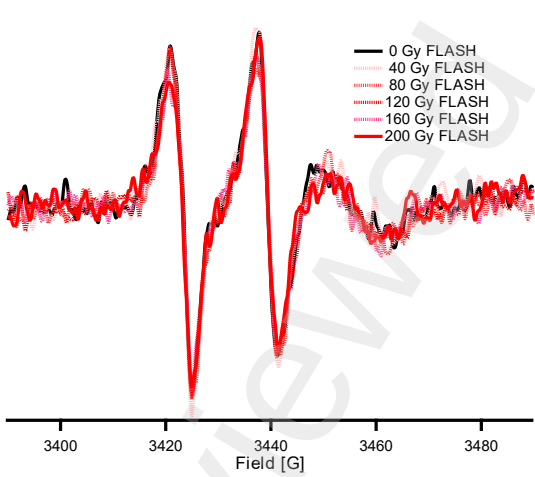

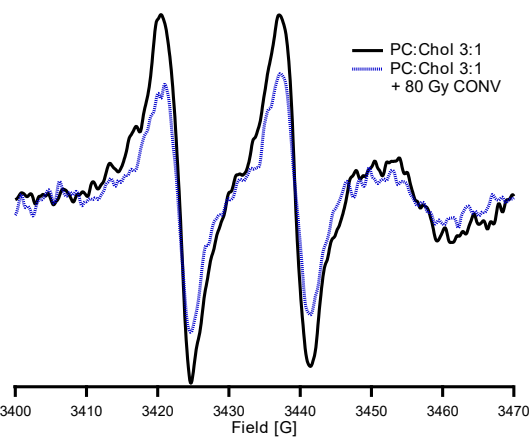

B

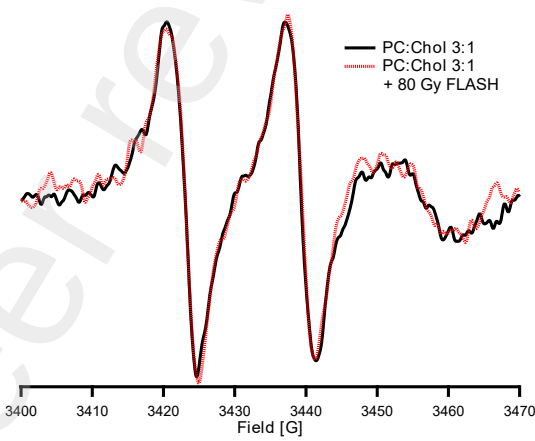

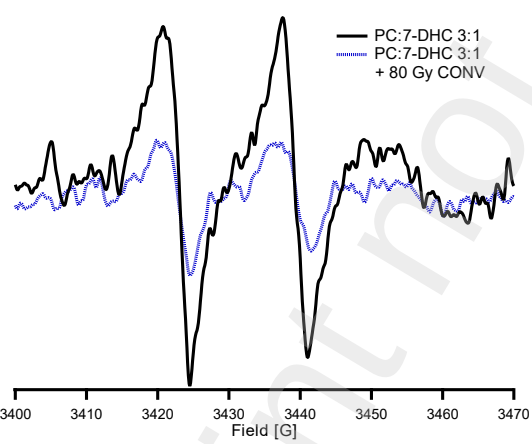

C

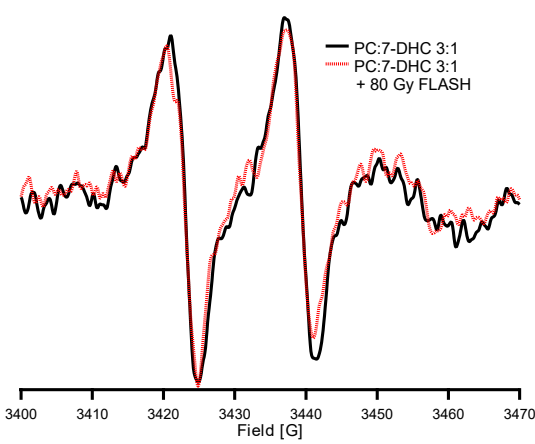

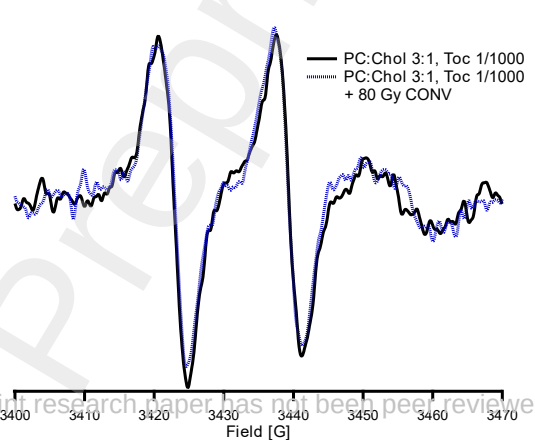

D

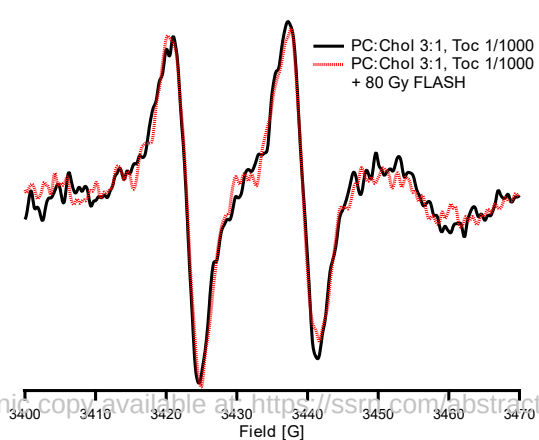

Table 1. Relative number of molecules of each lipid in the liposome formulations

	PC 18:2 60%	Chol	7-DHC	Toc
PC:Chol 3:1	3	1		
PC:Chol 1:1	1	1		
PC:7-DHC 3:1	3		1	
PC:Chol 3:1 Toc 1/2000	3	1		0.0015
PC:Chol 3:1 Toc 1/1000	3	1		0.003
PC:Chol 3:1 Toc 1/500	3	1		0.006
PC:Chol 3:1 Toc 1/200	3	1		0.015